Characterization of FimC, a Periplasmic Assembly Factor for Biogenesis of Type 1 Pili in *Escherichia coli*†

Uta Hermanns, Peter Sebbel, Verena Eggli, and Rudi Glockshuber*

Institut für Molekularbiologie und Biophysik, Eidgenössische Technische Hochschule Hönggerberg, CH-8093 Zürich, Switzerland

Received March 9, 2000; Revised Manuscript Received July 16, 2000

ABSTRACT: Assembly of type 1 pili from *Escherichia coli* is mediated by FimC, a periplasmic chaperone (assembly factor) consisting of two immunoglobulin-like domains. FimC is assumed to recognize the individual pilus subunits in the periplasm mainly via their conserved C-terminal segments and to deliver the subunits to an assembly platform in the outer membrane. Here we present the first biochemical characterization of a periplasmic pilus chaperone and analyze the importance of the two chaperone domains for stability and function. Comparison of the isolated C-terminal domain with wild-type FimC revealed a strongly reduced thermodynamic stability, indicating strong interdomain interactions. The affinity of FimC toward a peptide corresponding to the 11 C-terminal residues of the type 1 pilus adhesin FimH is at least 1000-fold lower compared to binding of intact FimH, confirming that bacterial pilus chaperones, unlike other chaperones, specifically interact with folded pilus subunits.

An important initial event during the establishment of infections by pathogenic Gram-negative enterobacteria is the attachment of bacteria to host cell receptors. This process is mediated by adhesive surface organelles termed pili or fimbriae (*1*−*4*). Pili are large, heterooligomeric protein filaments anchored to the bacterial outer membrane. Type 1 pili play an important role for the uropathogenicity of *Escherichia coli* strains. They enable the bacteria to bind to mannose-containing receptors at host cell surfaces (*3*) and enhance the virulence of pathogenic *E. coli* strains (*5*, *6*). Binding of type 1 pili to host cell receptors is accomplished by the adhesin FimH, a pilus subunit found at the tip and possibly in several copies along the pilus (*7*−*11*). In addition, type 1 pili also mediate survival and long-term persistence of uropathogenic *E. coli* strains inside macrophages and may thus contribute to the spontaneous reoccurrence of *E. coli* infections such as cystitis (*5*). For these reasons, type 1 pili are potential targets for the development of antibiotics, which, for example, prevent pilus assembly or inhibit adhesiveness. FimH also constitutes a promising vaccine for prevention of mucosal *E. coli* infections (*12*, *13*). Type 1 pili are 0.5−2 μm long and 7 nm wide filaments (*3*) composed of 500−3000 protein subunits. Overall, nine different *E. coli* proteins are involved in the biogenesis of type 1 pili, whose genes are clustered at 98 min of the *E. coli* K-12 chromosome (*3*, *14*). FimA, the main structural pilus subunit, comprises about 98% of all pilus proteins, while the residual 2% are comprised by FimF, FimG, the adhesin FimH, and possibly FimI (*3*). The outer membrane protein FimD anchors the pilus to the bacterial surface and represents its assembly platform, while the cytosolic proteins FimB and FimE regulate the transcription of pilus genes (*15*). Type 1 pilus assembly in vivo depends on FimC, a monomeric assembly factor (pilus chaperone) of 205 amino acids in the periplasm (*16*, *17*). FimC is assumed to form stoichiometric complexes with each of the five different subunits in the periplasm and to deliver the subunits to FimD. This oligomeric outer membrane protein allows translocation of the pilus subunits to the cell surface and their incorporation into the growing pilus (*1*, *3*, *4*, *18*−*20*). The three-dimensional structure of FimC in solution has been solved by nuclear magnetic resonance (NMR) spectroscopy (*21*) (Figure 1). The structure is similar to the crystal structure of the P pilus chaperone PapD (*22*) that shares 34% sequence identity with FimC. FimC consists of two globular domains (residues 1−115 and 131−205) with an immunoglobulin-like tertiary structure that are connected by a short linker peptide (residues 116−130) (*21*). Previous X-ray studies on complexes between PapD and synthetic peptides corresponding to the C-terminal residues of P pilus subunits PapG and PapK indicated that the conserved C-terminal octapeptide sequences of bacterial pilus subunits are an important common recognition motif of bacterial pilus chaperones (*23*, *24*). In these PapD/peptide complexes, the peptides are bound in an extended conformation to the N-terminal PapD domain in a β-sheetlike manner via hydrogen bonds. Their C-terminal carboxylates form charged hydrogen bonds with the invariant chaperone residues Arg8 and Lys112 (*23*, *24*). However, NMR studies on the 1:1 complex between FimC and the intact adhesin FimH have shown that the contact area between FimC and FimH is much larger than that identified in the structures of the PapD/peptide complexes (*25*). Specifically, there are approximately 30 additional residues from the N-terminal FimC domain that interact with FimH and do not correspond to peptide-binding residues in PapD. The recently solved X-ray structure of the FimC-FimH complex from *E. coli* has shown that FimH is a two-domain protein. The N-terminal domain contains the mannose-binding site of the adhesin, whereas the C-terminal domain exhibits homology to the other structural pilus subunits and possesses an immunoglobulin-like fold. FimC only binds to the C-terminal FimH

† This project was supported by the Schweizerischer Nationalfonds.

* To whom correspondence should be addressed. Phone: 41-1-633-6819. Fax: 41-1-633-1036. E-mail: rudi@mol.biol.ethz.ch.

10.1021/bi000549a CCC: $19.00 © 2000 American Chemical Society
Published on Web 09/01/2000

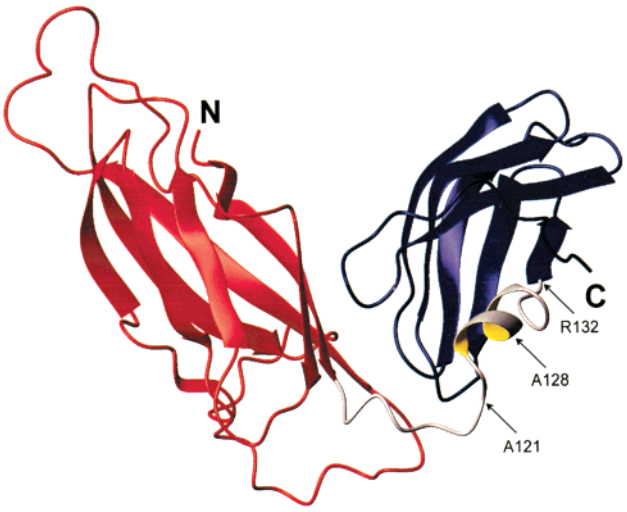

FIGURE 1: Ribbon drawing of the NMR structure of FimC. The N-terminal domain (residues 1−115) and the C-terminal domain (residue 131−205) are colored in red and blue, respectively. The domains are connected by a 15-residue linker peptide shown in gray that contains a small 3_{10}-helix (segment 126−130). The positions of the C-terminal residues of the FimC segments encoded by the plasmids pFimC-N and pFimC-N-L (Ala121 and Arg132, respectively), and the first amino acid of the cytoplasmically expressed C-terminal domain (Ala128) are indicated by arrows. The figure was generated with the program MOLMOL (*43*).

domain through a donor strand complementation mechanism in which strand G of the N-terminal chaperone domain completes the immunoglobulin-like fold of the pilin domain (*26*). There is no significant contribution of the C-terminal FimC domain to FimH binding. An analogous binding mode was found for the complex between PapD and the minor P pilus subunit PapK (*27*).

In this paper, we describe the first biochemical characterization of a bacterial pilus chaperone, using FimC as a model.

EXPERIMENTAL PROCEDURES

Materials. DE52 and CM52 cellulose were obtained from Whatman (Maidstone, U.K.). Phenyl superose, PD10, and Superdex 75 HR gel filtration columns were purchased from Pharmacia (Uppsala, Sweden). Tryptone and yeast extract were from Difco (Detroit). BIAcore chips were from BIAcore (Uppsala, Sweden).

Construction of Expression Plasmids. Molecular cloning techniques were based on Sambrook et al. (*28*). The gene coding for FimC (*17*) with its natural signal sequence and ribosomal binding site was amplified by the polymerase chain reaction (PCR) from the genome of the *E. coli* K12 wild-type strain W3110 (*29*) using the primers FimC1 (5′-ATT GTT CAG CAA AGC TTC TAG AAA CAG GAA CAG GAC AGT GAG TAA TAA-3′) and FimC2 (5′-CAA AAT GAC GGG CGT AAT GGA ATA AGG ATC CAA GCT TTT TTC GCC TG-3′). The gene was cloned via the *Xba*I and *Hin*dIII restriction sites into a derivative of pRBI-PDI-T7 (*30*) where *fimC* is under control of the T7 promoter/*lac* operator. The T7 terminator sequence from the vector pET11a (Stratagene) was introduced at the 3′ end of the *fimC* gene via the *Bam*HI and *Hin*dIII restriction sites, yielding the expression plasmid pFimC. For cytoplasmic production of the C-terminal FimC domain (residues 128−205) the *Nde*I−*Bam*HI fragment from pFimC-N containing the genetic sequence of the C-terminal domain without signal sequence and the T7 terminator was cloned into pRBI-PDI-T7-*Nde*I via *Nde*I and *Bam*HI, yielding pFimC-CsSS. pRBI-PDI-T7-*Nde*I was derived from pRBI-PDI-T7 by introduction of a *Nde*I site at the start codon of RBI. The plasmid pFimC-N for periplasmic expression of the N-terminal domain and cytoplasmic coexpression of the C-terminal domain was obtained by site-directed mutagensis according to Kunkel et al. (*31*) using single-stranded, uridinylated DNA of pFimC, the MutageneTM Kit from Bio-Rad (Herkules, CA) and the mutagenesis primer 5′-CCG GCT AAA TTA GCG TAA CTC GAG CAT GAA AGA GGG AGA CAT ATG GCA GAA AAA TTA AGA- 3′. The complete nucleotide sequences of the plasmids used in this paper has been deposited on our web site (http://www.mol.biol.ethz.ch/glockshuber/).

Expression and Purification of FimC and Its C-Terminal Domain. For production of FimC, cells of *E. coli* BL21-(DE3) (*32*) transformed with pFimC were grown at 25 °C in 10 L of LB medium containing ampicillin (100 μg/mL) (LB/amp) until an optical density at 600 nm (OD_{600}) of 1.0 was reached. After addition of IPTG (final concentration 1 mM) the culture was grown for another 16 h. The bacteria were harvested by centrifugation, resuspended at 4 °C in 100 mL of 50 mM Tris/HCl, pH 7.5, 150 mM NaCl, 5 mM EDTA, and 1 mg/mL polymyxin B sulfate, and stirred for 2 h at 4 °C. After centrifugation, the supernatant was dialyzed against 10 mM Tris/HCl, pH 8.0, and applied to a DE52 cellulose column. The column was washed with 10 mM Tris/HCl, pH 8.0, and the flow-through was applied to a CM52 cellulose column. FimC was eluted with a linear NaCl gradient in 10 mM Tris/HCl, pH 8.0. Fractions containing FimC were pooled, mixed with 4.0 M ammonium sulfate to a final concentration of 1.2 M ammonium sulfate, and applied to a phenyl superose column. FimC was eluted with a linear gradient from 1.2 to 0.5 M ammonium sulfate in 10 mM Tris/HCl, pH 8.0. Fractions with pure FimC were pooled, dialyzed against distilled water and stored at −20 °C.

For cytoplasmic expression of the C-terminal FimC domain, *E. coli* BL21(DE3) harboring pFimC-CΔSS was grown at 37 °C in 10 L of LB/amp medium and expression was induced with 1 mM IPTG at an OD_{600} of 0.5. After 3 h, the cells were harvested and subjected to periplasmic extraction as described above. The spheroblasts were disrupted in a French pressure cell (18 000 PSI) after suspension in 200 mL of 50 mM Tris/HCl, pH 7.5, 0.5 mM β-mercaptoethanol, 5 mM EDTA. The inclusion bodies were washed with 1% Triton X-100 and solubilized in 150 mL of 9.0 M urea, 10 mM Mops/NaOH, pH 7.0. Insoluble material was removed by centrifugation, and the supernatant was diluted to 4.0 M urea and applied to a DE52 cellulose column connected to a CM52 cellulose column in 4.0 M urea, 10 mM Mops/NaOH, pH 7.0. The flow-through containing the C-terminal domain was dialyzed against 50 mM sodium phosphate, pH 7.0, concentrated, and applied to a Superdex 75 gel filtration column. Fractions containing the pure C-terminal domain were combined, dialyzed against distilled water and lyophilized. The molecular mass of purified FimC was confirmed by MALDI mass spectrometry (calculated, 22 729.9 Da; measured, 22 720.0 Da).

Protein Concentration. Protein concentrations were determined by the specific absorbance at 280 nm ($A_{280nm,1cm,1mg/mL}$) with values of 1.07 for FimC, 0.567 for the C-terminal FimC domain, and 1.08 for the FimC/FimH complex (*33*).

Analytical Gel Filtration. Analytical gel filtration of FimC and its C-terminal domain was performed on a Superdex 75 HR column in 50 mM sodium phosphate, pH 7.0 at a flow rate of 10 mL/h. The FimC/FimH complex was prepared as described previously (*25*). Analytical gel filtration of the FimC/FimH complex was performed under the same conditions used for peptide-binding studies (25 °C, PBS buffer, pH 8.0). The FimC/FimH complex was diluted with PBS to concentrations of 8.6−0.3 μM and incubated at 25 °C for at least 2 h. Samples of 50 μL were applied to a Superdex 75 HR column. Eluted proteins were detected by their absorbance at 280 nm. The apparent molecular mass of the FimC/FimH complex in PBS buffer was 42 ± 9 kDa.

Circular Dichroism and Fluorescence Spectroscopy. Far-UV and near-UV circular dichroism (CD) spectra were recorded on a JASCO J-710 CD spectropolarimeter at protein concentrations of 1 mg/mL in 10 mM sodium phosphate, pH 7.0 at 25 °C. For far-UV CD and near-UV CD measurements, 0.2 and 10 mm cuvettes were used, respectively. All fluorescence measurements were performed on a HITACHI F 4500 fluorescence spectrometer at 25 °C.

Urea-Induced Unfolding Equilibria and Stopped-Flow Measurements. Unfolding/refolding equilibria of FimC and its C-terminal domain were measured at 25 °C and a constant ionic strength of 92 mM (calculated according to ref *34*). The following buffers containing different concentrations of urea were used. At pH 7.0, 50 mM sodium phosphate; at pH 4.0, 50 mM formic acid/NaOH and 57 mM sodium chloride; at pH 2.0: 50 mM sodium phosphate and 68 mM sodium chloride. The native or unfolded proteins (in 6.0 M urea) were diluted with the above buffers to a final protein concentration of 1.0 μM in the case of FimC and to a concentration of 2.8 μM in the case of the C-terminal domain, and incubated at 25 °C for 3 days. Equilibrium transitions were followed by the protein fluorescence at 335 nm (excitation at 295 nm) in the case of FimC and at 302 nm (excitation at 280 nm) in the case of the C-terminal domain. Data were evaluated according to the two-state model of folding (*35*) using a six-parameter fit (*36*) and normalized. The urea dependence of the apparent rate constant of unfolding and refolding of the C-terminal domain were measured fluorimetrically with a SX-17MV stopped-flow reaction analyzer (Applied Photophysics, Leatherhead, U.K.) at 25 °C in 50 mM sodium phosphate, pH 7.0. The native or urea-denatured protein (in 3.0 M urea) was diluted 1:11 to a final protein concentration of 5.0 μM with 50 mM sodium phosphate, pH 7.0, containing different concentrations of urea. The fluorescence intensity above 305 nm (excitation at 280 nm) was recorded for 0.5 s and the fluorescence traces were analyzed according to a single first-order reaction. The urea dependence of the averaged apparent first-order rate constants was evaluated according to the equation

$$\ln k_{app} = \ln[k_f^{H_2O} \exp(-m_f[\text{urea}]) + k_u^{H_2O} \exp(m_u[\text{urea}])],$$

where k_{app} is the apparent rate constant of folding/unfolding, $k_f^{H_2O}$ and $k_u^{H_2O}$ are the rate constants of folding and unfolding in the absence of denaturant, respectively, m_f and m_u give the linear dependence of ln k_f and ln k_u on the denaturant concentration and [urea] is the concentration of urea (*37*).

Peptide-Binding Measurements. Peptide binding of FimC was investigated with a synthetic peptide consisting of the C-terminal 11 residues of the pilus subunit FimH extended by a hydrophilic N-terminal tetrapeptide (S-R-R-S) (overall sequence: H_3N^+-S-R-R-S-*Q-S-I-I-G-V-T-F-V-Y-Q*-CO_2^-). The peptide was biotinylated at its free N-terminus by mixing with D-biotinyl-ϵ-aminocaproic acid *N*-hydroxysuccinimide ester (Boehringer Mannheim, Germany) at a 1:1 ratio (concentrations of 0.2 mM each) in 50 mM sodium phosphate, pH 8.0, 100 mM NaCl, 0.1 mM EDTA, and incubation for 1 h at room temperature. Peptide-binding experiments were performed on a BIAcore surface plasmon resonance instrument (Pharmacia Biosensor AB) at 25 °C in PBS buffer using a microsensor chip covalently coated with streptavidin. A total of 10 μL of a 20 μM solution of the biotinylated peptide was injected at a flow rate of 5 μL/min to allow binding of the peptide to the sensor chip. After washing with PBS, the chip was equilibrated with 10 μL of a solution of FimC (1−100 μM) in PBS and then washed with PBS, and the amplitude of the first-order signal decrease during recovery of the baseline was recorded for all FimC concentrations after washing for 10 s. The apparent dissociation constant (K_D^{app}) of the FimC/peptide complex was deduced by fitting the data according to the equation

$$S = S_F/(1 + [\text{FimC}]/K_D^{app}) + S_B[1 - (1/(1 + K_D^{app}/[\text{FimC}]))],$$

where S is the resonance signal after washing for 10 s, S_F is the signal in the absence of FimC, S_B is the signal after washing for 10 s when all binding sites are occupied by FimC before washing, and [FimC] is the concentration of FimC in solution prior to washing. It was verified that no direct binding of FimC to streptavidin occurred.

RESULTS

Expression and Purification of FimC and Its C-Terminal Domain. FimC was overproduced in *E. coli* and purified to homogeneity by conventional chromatography with yields of 30 mg FimC/liter of bacterial culture (Figure 2A). To study the influence of domain interactions on the stability of FimC in vitro, we intensively tried also to produce milligram quantities of the isolated N-terminal domain (residues 1−121; pFimC-N), the N-terminal domain extended by the linker peptide (residues 1−132; pFimC-N-L) and the isolated C-terminal domain (residues 128−205; pFimC-C) (Figure 1) under control of the T7 promoter/*lac* operator system in the periplasm of *E. coli* BL21(DE3). However, none of the domains could be detected in the periplasmic or insoluble fractions at growth temperatures between 25 and 37 °C (data not shown). To overcome this problem, we removed the bacterial signal sequences and tried to express the isolated FimC domains in the cytoplasm of BL21(DE3). Only the isolated C-terminal domain (FimC-C) could be obtained in reasonable amounts and was purified from inclusion bodies with a yield of 15 mg of pure FimC-C/L of bacterial culture (Figure 2A). In contrast, cytoplasmic expression of the N-terminal domain constructs again could not even be detected after immunoblotting (data not shown). Limited proteolysis of FimC using subtilisin, proteinase K, thrombin, and trypsin also did not yield fragments corresponding to the N-terminal domain of FimC (data not shown). Analysis of FimC and the isolated C-terminal FimC domain by analytical gel filtration experiments revealed molecular masses of 27 (± 5) kDa for FimC and 8 (±5) kDa for FimC-C, corresponding to the monomeric states of both proteins (Figure 2B).

Folding and Thermodynamic Stability of FimC and Its Isolated C-Terminal Domain. For further characterization of

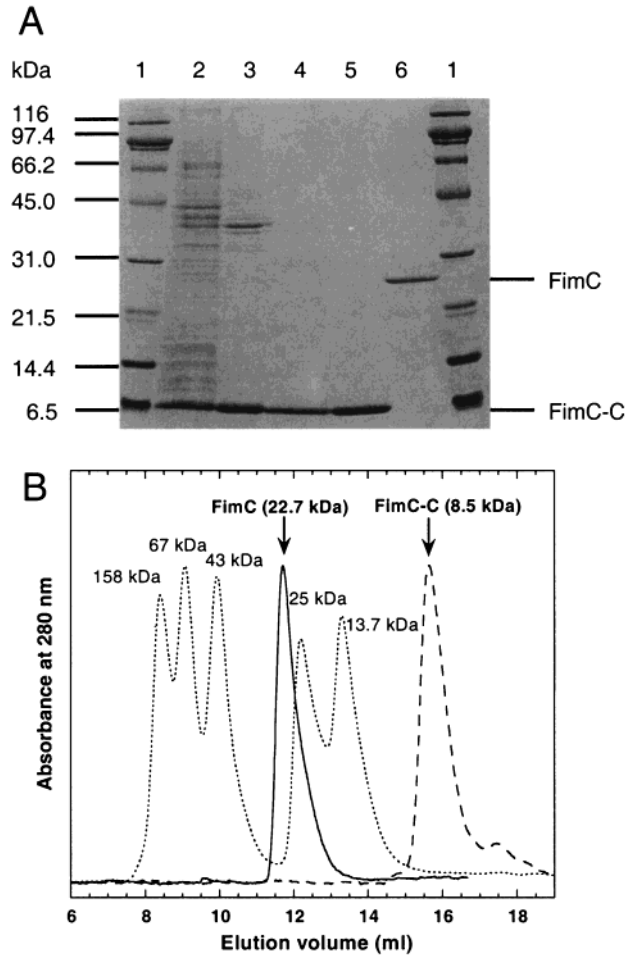

FIGURE 2: FimC and its isolated C-terminal domain (residues 128−205) are monomers. (A) Purification of the C-terminal FimC domain from cytoplasmic inclusion bodies. A reducing 17% (w/v) polyacrylamide−SDS gel stained with Coomassie Blue is shown. Lane 1, molecular mass standard; lane 2, total cell extract of induced cells of *E. coli* BL21(DE3)/pFimC-CΔSS; lane 3, insoluble fraction of the cell extract; lane 4, pooled fractions after solubilization and chromatography on DE52 cellulose and CM52 cellulose in the presence of 4.0 M urea; lane 5, purified C-terminal domain after refolding and gel filtration on Superdex 75 under native conditions; lane 6, purified FimC. (B) Analytical gel filtration of FimC and its C-terminal domain on a Superdex 75 column (30 × 1 cm) in 50 mM sodium phosphate (pH 7.0) at 22 °C. FimC (solid line) and the C-terminal domain (dashed line) were applied at concentrations of 20 μM and 100 μM, respectively. The dotted line corresponds to a mixture of proteins used as molecular mass standards. Proteins were detected by their absorbance at 280 nm.

the C-terminal domain, its spectroscopic properties were compared with those of wild-type FimC. As expected for a β-sheet protein, the far-UV circular dichroism (CD) spectrum of FimC shows a minimum at 217 nm (molar mean residue ellipticity −5300 deg cm^2 dmol^{-1}) (Figure 3A). However, the spectrum exhibits an unusual second minimum at 195 nm. This is almost certainly due to the intrinsic spectroscopic properties of the C-terminal domain, which lacks the β-sheet-specific minimum around 215 nm and displays a strong minimum at 196 nm (Figure 3A). The presence of a defined tertiary structure in the isolated C-terminal domain is, however, evident from a characteristic fine structure with positive ellipticity in its near-UV CD spectrum, whereas the near-UV CD spectrum of FimC shows negative ellipticity (Figure 3B). Both tryptophan residues of FimC (Trp36 and Trp84) are located in the N-terminal domain (*21*, *25*). In accordance with the NMR structure of FimC, its fluorescence maximum at 345 nm indicates that the tryptophans are partially solvent exposed. As expected, the isolated C-terminal domain exhibits a pure tyrosine fluorescence spectrum (maximum at 304 nm) (Figure 3C). The fluorescence intensity of both FimC and its C-terminal domain decreases significantly after unfolding of the proteins by 6.0 M urea (Figure 3C). Urea-induced unfolding of FimC at pH 7.0 and 4.0, followed by fluorescence, yielded cooperative one-step transitions that were fully reversible (Figure 4). Evaluation of the data according to the two-state model of folding yielded free energies of folding of −38.2 and −32.7 kJ/mol, respectively (Table 1). The corresponding *m*-values of 12.8 and 11.4 kJ mol^{-1} M^{-1} are slightly higher than the expected *m*-value of 9.9 kJ mol^{-1} M^{-1} for an urea-induced two-state transition of a 205 residue protein (*38*).

The isolated C-terminal FimC domain also showed completely reversible unfolding transitions and proved to be strongly destabilized compared to FimC. The domain is only marginally stable with a free energy of folding of −4.2 kJ/mol at pH 7.0 (Figure 5A, Table 1). The apparent rate constants of unfolding and refolding of the C-terminal FimC domain at pH 7.0 and different urea concentrations, measured with stopped-flow tyrosine fluorescence, were consistent with two-state folding and reproduced the equilibrium measurements within experimental error (Figure 5B, Table 1). The C-terminal FimC domain lacks cis-prolines (*21*), and the fluorescence traces obtained for the unfolding and refolding reactions could be described by single-exponential functions at all urea concentrations. In addition, no rapid burst phases within the dead time of the stopped-flow measurement (2 ms) were observed, indicating the absence of a hydrophobic collapse prior to tertiary structure formation of the C-terminal domain. The slopes of the folding and unfolding branches in Figure 5B showed that the transition state of folding of the C-terminal domain is closer to the native than to the unfolded state ($\alpha = 0.68$). Extrapolation of the folding and unfolding branches in Figure 5B to 0 M urea yields 15 s^{-1} for the rate constant of folding and 3.4 s^{-1} for the rate constant of unfolding. Refolding of intact FimC at pH 7.0, monitored by the increase in tryptophan fluorescence, revealed complex, multiphasic kinetics with one slow folding phase ($t_{1/2} \approx 100$ s), consistent with the expected slow folding rate due to the cis Thr51−Pro52 peptide bond in the N-terminal FimC domain (*21*) (data not shown).

FimC Only Weakly Binds to the C-Terminal Peptide of the Type 1 Pilus Adhesin FimH. To study the affinity of FimC to the C-terminal segments of type 1 pilus subunits, we focused on the C-terminal peptide of the type 1 pilus adhesin FimH for a comparison with the extraordinarily stable complex between FimC and intact FimH (*25*, *26*). For this purpose, a synthetic peptide corresponding to the C-terminal 11 residues of FimH, extended by the tetrapeptide Ser-Arg-Arg-Ser at the N-terminus to increase solubility, was used. The peptide was then biotinylated at the free N-terminus and coupled to a BIAcore sensor chip coated with streptavidin. The chip was purged with buffer containing different concentrations of FimC, and the amount of bound FimC at the different FimC concentrations was determined by surface plasmon resonance (Figure 6). The binding data at pH 8.0 and 25 °C were consistent with a single chemical binding equilibrium, yielding an apparent dissociation con-

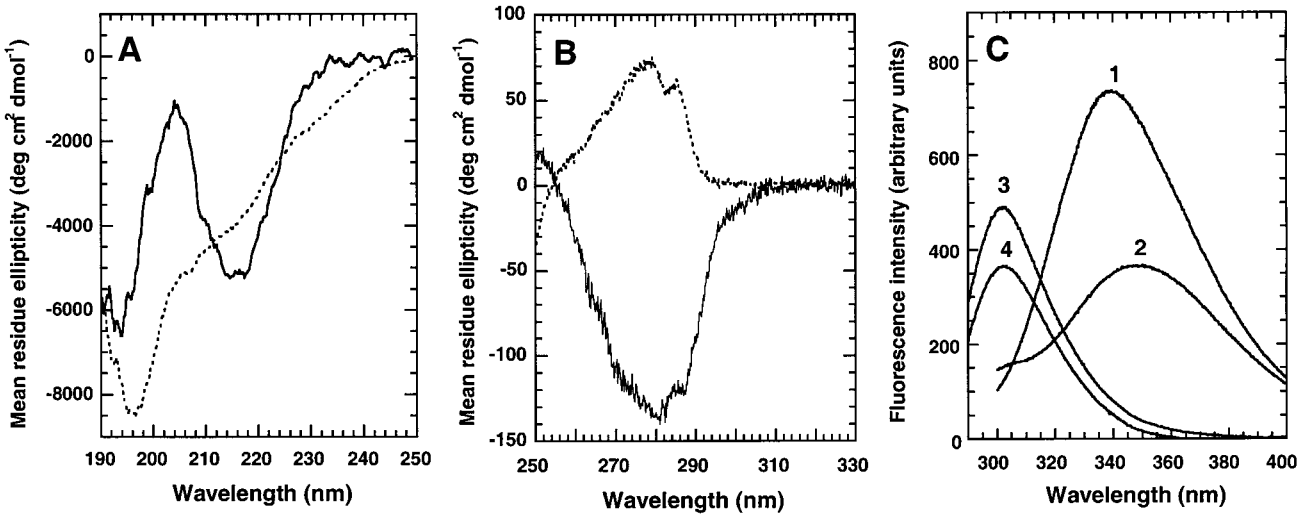

FIGURE 3: Spectroscopic characterization of FimC and its C-terminal domain. (A) Far-UV and (B) near-UV circular dichroism spectra of FimC (solid lines) and its C-terminal domain (dotted lines) at 25 °C in 10 mM sodium phosphate, pH 7.0. (C) Fluorescence emission spectra of FimC and its C-terminal domain. (1) Native FimC, (2) unfolded FimC in 6.0 M urea (excitation at 295 nm), (3) native C-terminal domain, (4) unfolded C-terminal domain in 6.0 M urea (excitation at 280 nm). Protein concentrations were 1 μM for FimC and 2.8 μM for the C-terminal domain.

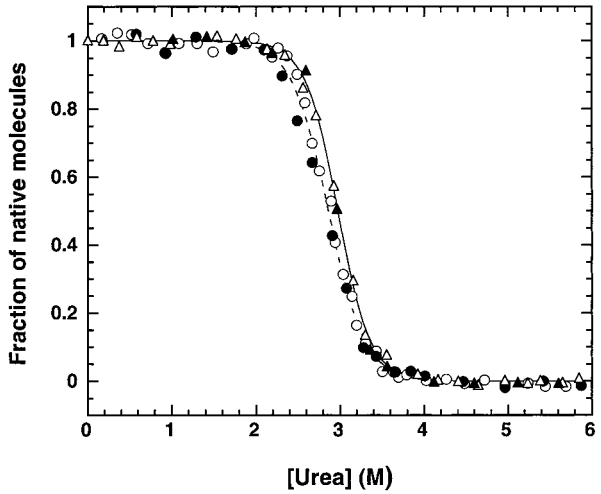

FIGURE 4: Urea-dependent unfolding/refolding equilibria of FimC at pH 4.0 (circles) and at pH 7.0 (triangles) (25 °C), followed by fluorescence emission at 335 nm (excitation at 295 nm). Unfolding and refolding experiments are represented by open and closed symbols, respectively. The original fluorescence data were fitted according to the two-state-model and normalized (pH 7.0, solid line; pH 4.0, dashed line).

stant (K_D) of 8 ± 1 μM (Figure 6). In contrast, no binding of the isolated C-terminal FimC domain to the C-terminal FimH peptide could be observed, in accordance with the lack of corresponding contacts in the FimC-FimH crystal structure (*26*). As FimH tends to aggregate in the absence of FimC, it could not be coupled efficiently to the BIAcore chip. Therefore, the stability of the intact FimC/FimH complex against dissociation was investigated by analytical gel filtration under the same conditions. The concentration of the complex in the applied sample was gradually decreased in a set of gel filtration runs. No significant dissociation of the complex could be detected at concentrations as low as 0.3 μM in the applied sample and 20 nM in the elute (data not shown). Consequently, the K_D of the complex must be below 10 nM. Binding of the C-terminal FimH peptide to FimC is thus at least 1000-fold weaker compared to binding of intact FimH.

Table 1: Thermodynamic Stabilities of FimC and Its C-terminal Domain (FimC-C) at 25 °C Deduced Form Urea-Dependent Equilibrium Transitions and Stopped-Flow Fluorescence Measurements

	ΔG (kJ mol^{-1})	cooperativity (*m*-value) (kJ mol^{-1} M^{-1})	midpoint of transition (M urea)
FimC, pH 7.0	−38.2 ± 1.3	12.8 ± 0.4	3.0 ± 0.2
FimC, pH 4.0	−32.7 ± 1.8	11.4 ± 0.6	2.7 ± 0.3
FimC-C, pH 7.0	−4.2 ± 0.9	4.6 ± 0.3	0.9 ± 0.3
FimC-C, pH 7.0, stopped flow kinetics[a]	−3.7 ± 0.3	5.3 ± 0.5	0.7 ± 0.1

[a] Fitting the data in Figure 5B according to the two-state model yields values of 15.1 ± 1.1 s^{-1} and 3.4 + 0.2 s^{-1} for the rate constants of folding ($k_f^{H_2O}$) and unfolding ($k_u^{H_2O}$) in the absence of urea, respectively. The slopes of the linear dependence of the logarithm of k_f and k_u on urea concentration (Figure 5B) have the following values: m_f = −1.45 ± 0.2 M^{-1}; m_u = 0.68 ± 0.02 M^{-1}. The equation $m = (m_u - m_f)RT$ yields the calculated m-value for the equilibrium transition (5.3 ± 0.5 kJ mol^{-1} M^{-1}), which agrees within experimental error with the equilibrium measurement (4.6 ± 0.5 kJ mol^{-1} M^{-1}). The α-value of 0.68, calculated from $\alpha = |m_f|/(|m_f| + |m_u|)$, indicates that the transition state of folding is closer to the native than to the unfolded state.

DISCUSSION

The assembly factor FimC has been identified as an essential component for the formation of adhesive type 1 pili (*16*, *17*). As a prerequisite for future studies on the in vitro reconstitution of type 1pili in the presence of FimC, we describe here the biochemical and biophysical properties of FimC and its isolated C-terminal domain. Several lines of evidence indicate that the interactions between both immunoglobulin-like domains of FimC are essential for the overall thermodynamic stability of the chaperone and its stability against degradation in vivo. While the isolated N-terminal domain appears to be so unstable that it cannot be overexpressed in *E. coli*, the isolated C-terminal domain could be purified, and its stability was compared with that of FimC. Although the C-terminal FimC domain is an autonomous folding unit, it proved to be an extremely unstable protein (ΔG = −4.2 kJ mol^{-1}) with a significant fraction of the domain already unfolded in the absence of denaturant. In contrast, intact FimC is an about 10-fold more

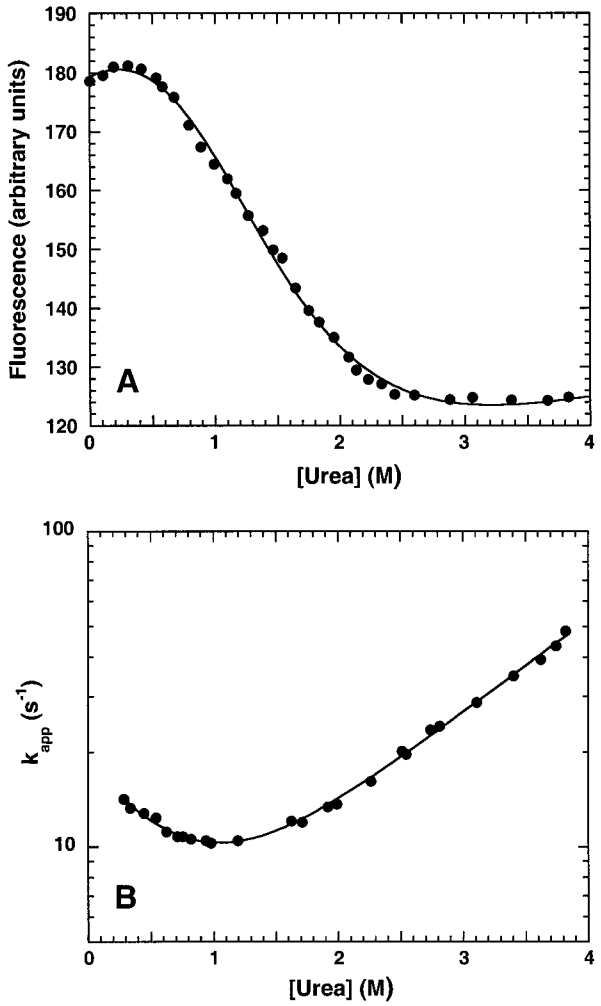

FIGURE 5: Urea-dependent unfolding/refolding equilibrium of the C-terminal FimC domain at pH 7.0 at 25 °C, measured by tyrosine fluorescence (excitation at 280 nm). (A) Equilibrium unfolding transition. The solid line corresponds to a two-state analysis (B) Urea dependence of the apparent rate constant (k_{app}) of unfolding and refolding of the C-terminal domain measured by stopped-flow tyrosine fluorescence. The urea-dependence of k_{app} was fitted according to the two-state model (solid line).

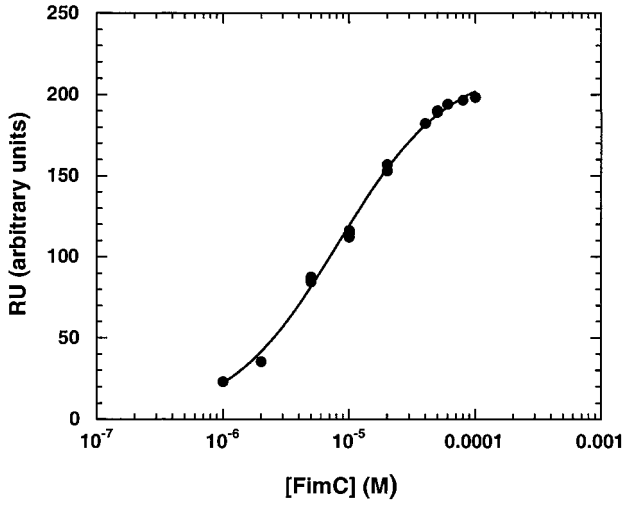

FIGURE 6: Determination of the apparent dissociation constant (K_D^{app}) of the complex between FimC and the peptide H_3N^+-S-R-R-S-*Q-S-I-I-G-V-T-F-V-Y-Q-CO*$_2$ containing the 11 C-terminal residues of FimH (italics). The peptide was biotinylated at its N-terminus and immobilized on a BIAcore sensor chip coated with streptavidin. The binding of FimC to the peptide was measured at pH 8.0 and 25 °C. The chip was equilibrated with a solution of FimC (1−100 μM), then washed with buffer and the amplitude of the signal change during recovery of the baseline [given in resonance units (RU)] after 10 s of washing was determined. The solid line corresponds to a fit according to a single chemical binding equilibrium.

stable protein, with a free energy of folding of −38.2 kJ mol^{-1} at pH 7.0. FimC is thus composed of two comparably unstable modules, and the interdomain contacts are the most important interactions that contribute to its thermodynamic stability. The importance of the interdomain interactions is also evident from a well-defined hydrophobic core between both domains and the highly conserved salt bridge formed by the residues Glu80, Arg116, and Asp192 in the solution structure of FimC (*21*). The two-domain architecture of periplasmic pilus chaperones could have been a special advantage during the evolution of these highly specific binding proteins. Destabilizing mutations in individual chaperone domains occurring during evolution toward their actual function could have been compensated by mutations that strengthened the interaction between the domains. Obviously, the mutual domain stabilization in FimC has developed to a point where individual domain unfolding does no longer occur and the whole protein unfolds in a single two-state transition. This is clearly evident from the cooperativites of folding observed for FimC (12.8 and 11.4 kJ mol^{-1} M^{-1} at pH 7.0 and 4.0, respectively), which are even higher than the expected value of 9.9 kJ mol^{-1} M^{-1} for an urea-induced two-state unfolding transition of a 205 residue protein (*38*). An analogous example in this context is γB Crystallin from the vertebrate eye lens. This protein also mainly recruits its enormous stability from interdomain interactions. γB Crystallin evolved by gene duplication and fusion of two homologous β-sheet domains, but the isolated domains are much less stable than the intact protein (*39*, *40*).

Recently, the interactions between FimC and FimH have been characterized by TROSY−NMR in solution (*25*) and X-ray crystallography (*26*). In contrast to previous studies on complexes between PapD and synthetic peptides corresponding to the C-terminal residues of P-pilus subunits (*19*, *22*), it was found that the surface area of FimC covered by FimH is much larger, and that FimC very specifically interacts with the folded form of the adhesin. In the X-ray structure of the FimC/FimH complex the adhesin FimH is folded into two domains, the N-terminal lectin domain and the C-terminal pilin domain which is supposed to anchor the adhesin domain to the pilus. In the FimC/FimH complex, only the pilin domain of FimH interacts with FimC. The contact between the C-terminal β-strand of the pilin domain and FimC involves β-sheet hydrogen bonding to the G1 strand of FimC, which completes a lacking β-strand in the immunoglobulin-like pilin fold (*26*). The low affinity (apparent K_D = 8 μM) of FimC for the C-terminal FimH peptide, and the at least 1000-fold higher affinity toward the intact, folded FimH found in this study are in good agreement with these structural data which revealed multiple FimC/FimH contacts in addition to binding of the C-terminal FimH β-strand (*25*−*27*). Our gel filtration experiments showed that the purified complex does not dissociate when it is applied at concentrations of 0.3 μM and eluted at concentrations of 20 nM. This is in line with a previous study on the binding of the FimC/FimH complex to FimD, where no dissociation of the complex at concentrations as low as 75 nM was

observed (*20*). We are aware of the fact that the affinities of FimC toward intact FimH and C-terminal FimH peptide were measured with different methods, and that apparent K_D values obtained with BIAcore measurements are not necessarily identical to K_D values in solution. However, K_D values measured with BIAcore are generally lower compared to the values in solution due to rebinding effects and high local ligand concentrations on the chip (*41*). Therefore, binding of the C-terminal peptide may even be more than 1000-fold weaker compared to binding of the intact adhesin.

The low affinity of FimC for the C-terminal FimH peptide also has implications for the folding of individual pilus subunits in that it questions that FimC already interacts with unfolded pilus subunits prior to subunit folding, as suggested by Soto et al. (*20*). FimC rather appears to maintain folded subunits in a translocation- and assembly-competent tent state in the periplasm, and prevent premature association of folded subunits in the periplasm (*42*). On the other hand, however, the strong interaction between FimC and intact, folded FimH raises the question of how an efficient dissociation of the FimC/FimH complex is accomplished in vivo when FimC delivers the adhesin to the assembly platform FimD in the outer bacterial membrane. As the assembly of a complete pilus in *E. coli* occurs within 1−3 min (*3*), it seems that the FimC/FimH complex is less stable in vivo. The most likely mechanism for an induced dissociation of the complex seems to be a conformational change in the complex triggered by a specific contact with FimD.

ACKNOWLEDGMENT

We thank Jens Hennecke for his help during construction of the expression plasmids, Gerhard Frank for N-terminal sequencing and Peter James for recording mass spectra.

REFERENCES

1. Hultgren, S. J., Abraham, S. N., Caparon, M., Falk, P., St. Geme, III, J. W., and Normark, S. (1993) *Cell 73*, 887−901.
2. Hultgren, S. J., Jones, C. H., and Normark, S. (1996) in *Escherichia coli and Salmonella* (Neidhardt, F. C., Ed.) pp 2730−2756, ASM Press.
3. Klemm, P., and Krogfelt, K. A. (1994) in *Fimbriae* (Klemm, P., Ed.) pp 9−26, CRC Press Inc.
4. Soto, G. E., and Hultgren, S. J. (1999) *J. Bacteriol. 181*, 1059−1071.
5. Baorto, D. M., Gao, Z., Malaviya, R., Dustin, M. L., van der Merwe, A., Lublin, D. M., and Abraham, S. N. (1997) *Nature 389*, 636−639.
6. Connell, H., Agace, W. W., Klemm, P., Schembri, M. A., Marild, S., and Svanborg, C. (1996) *Proc. Natl. Acad. Sci. U.S.A. 93*, 9827−9832.
7. Abraham, S. N., Sun, D., Dale, J. B., and Beachey, E. H. (1988) *Nature 336*, 682−684.
8. Jones, C. H., Pinkner, J. S., Roth, R., Heuser, J., Nicholes, A. V., Abraham, S. N., and Hultgren, S. J. (1995) *Proc. Natl. Acad. Sci. U.S.A. 92*, 2081−2085.
9. Krogfelt, K. A. (1991) *Rev. Infect. Dis. 13*, 721−735.
10. Mulvey, M. A., LopezBoado, Y. S., Wilson, C. L., Roth, R., Parks, W. C., Heuser, J., and Hultgren, S. J. (1998) *Science 282*, 1494−1497.
11. Wu, X. R., Sun, T. T., and Medina, J. J. (1996) *Proc. Natl. Acad. Sci. U.S.A. 93*, 9630−9635.
12. Langermann, S., Palaszynski, S., Barnhart, M., Auguste, C. G., Pinkner, J. S., Burlein, J., Barren, P., Koenig, S., Leath, S., Jones, C. H., and Hultgren, S. J. (1997) *Science 276*, 607−611.
13. Langermann, S., Mollby, R., Burlein, J. E., Palaszynski, S. R., Auguste, C. G., DeFusco, A., Strouse, R., Schenerman, M. A., Hultgren, S. J., Pinkner, J. S., Winberg, J., Guldevall, L., Soderhall, M., Ishikawa, K., Normark, S., and Koenig, S. (2000) *J. Infect. Dis. 181*, 774−778.
14. Blattner, F. R., Plunkett, G., Bloch, C. A., Perna, N. T., Burland, V., Riley, M., ColladoVides, J., Glasner, J. D., Rode, C. K., Mayhew, G. F., Gregor, J., Davis, N. W., Kirkpatrick, H., Goeden, M. A., Rose, D. J., Mau, B., and Shao, Y. (1997) *Science 277*, 1453−1462.
15. Klemm, P. (1986) *EMBO J. 5*, 1389−1394.
16. Jones, C. H., Pinkner, J. S., Nicholes, A. V., Slonim, L. N., Abraham, S. N., and Hultgren, S. J. (1993) *Proc. Natl. Acad. Sci. U.S.A. 90*, 8397−8401.
17. Klemm, P. (1992) *Res. Microbiol. 143*, 831−838.
18. Dodson, K. W., Jacob-Dubuisson, F., Striker, R. T., and Hultgren, S. J. (1993) *Proc. Natl. Acad. Sci. U.S.A. 90*, 3670−3674.
19. Jacob-Dubuisson, F., Striker, R. T., and Hultgren, S. J. (1994) *J. Biol. Chem. 269*, 12447−12455.
20. Saulino, E. T., Thanassi, D. G., Pinkner, J. S., and Hultgren, S. J. (1998) *EMBO J. 17*, 2177−2185.
21. Pellecchia, M., Guntert, P., Glockshuber, R., and Wüthrich, K. (1998) *Nat. Struct. Biol. 5*, 885−890.
22. Holmgren, A., and Brändèn, C. I. (1989) *Nature 342*, 248−251.
23. Kuehn, M. J., Ogg, D. J., Kihlberg, J., Slonim, L. N., Flemmer, K., Bergfors, T., and Hultgren, S. J. (1993) *Science 262*, 1234−1241.
24. Soto, G. E., Dodson, K. W., Ogg, D., Liu, C., Heuser, J., Knight, S. D., Kihlberg, J., Jones, C. H., and Hultgren, S. J. (1998) *EMBO J. 17*, 6155−6167.
25. Pellecchia, M., Sebbel, P., Hermanns, U., Wüthrich, K., and Glockshuber, R. (1999) *Nat. Struct. Biol. 6*, 336−339.
26. Choudhury, D., Thompson, A., Stojanoff, V., Langermann, S., Pinkner, J., Hultgren, S. J., and Knight, S. D. (1999) *Science 285*, 1061−6.
27. Sauer, F. G., Futterer, K., Pinkner, J. S., Dodson, K. W., Hultgren, S. J., and Waksman, G. (1999) *Science 285*, 1058−61.
28. Sambrook, J., Fritsch, E. F., and Maniatis, T. (1989) *Molecular Cloning: A Laboratory Manual*, Cold Spring Harbor Laboratory Press, Plainview, NY.
29. Bachmann, B. J. (1972) *Bacteriol. Rev. 36*, 525−557.
30. Strobl, S., Muhlhahn, P., Bernstein, R., Wiltscheck, R., Maskos, K., Wunderlich, M., Huber, R., Glockshuber, R., and Holak, T. A. (1995) *Biochemistry 4*, 8281−8293.
31. Kunkel, T. A., Roberts, J. D., and Zakour, R. A. (1987) *Methods Enzymol. 154*, 367−382.
32. Studier, F. W., and Moffatt, B. A. (1986) *J. Mol. Biol. 189*, 113−130.
33. Gill, S. C., and van Hippel, P. H. (1989) *Anal. Biochem. 182*, 319−326.
34. Beynon, R. J., and Easterby, J. S. (1996) *Buffer Solutions: The Basics*, England, Oxford.
35. Pace, C. N. (1986) *Methods Enzymol. 131*, 266−280.
36. Santoro, M. M., and Bolen, D. W. (1988) *Biochemistry 27*, 8063−8068.
37. Jackson, S. E., and Fersht, A. R. (1991) *Biochemistry 30*, 10428−10435.
38. Myers, J. K., Pace, C. N., and Scholtz, J. M. (1995) *Protein Sci. 4*, 2138−2148.
39. Mayr, E. M., Jaenicke, R., and Glockshuber, R. (1997) *J. Mol. Biol. 269*, 260−269.
40. Mayr, E. M., Jaenicke, R., and Glockshuber, R. (1994) *J. Mol. Biol. 235*, 84−88.
41. Hung, D. L., and Hultgren, S. J. (1998) *J. Struct. Biol. 124*, 201−220.
42. Neri, D., Montigiani, S., and Kirkham, P. (1996) *Trends Biotechnol. 14*, 465−470.
43. Koradi, R., Billeter, M., and Wüthrich, K. (1996) *J. Mol. Graphics 14*, 52−55.

BI000549A